COLD SPRING HARBOR
Molecular Case Studies

RESEARCH REPORT

WP1066 induces cell death in a schwannomatosis patient–derived schwannoma cell line

Abdulrahman Allaf,[1] Berta Victoria,[1] Rosa Rosario,[1] Carly Misztal,[2] Sakir Humayun Gultekin,[3] Christine T. Dinh,[2] and Cristina Fernandez-Valle[1]

[1]Burnett School of Biomedical Sciences, College of Medicine, University of Central Florida (UCF), Orlando, Florida 32816, USA; [2]Department of Otolaryngology, [3]Department of Pathology, University of Miami Miller School of Medicine, Miami, Florida 33136, USA

Abstract Schwannomatosis is a rare genetic disorder that predisposes individuals to development of multiple schwannomas mainly in spinal and peripheral nerves and to debilitating chronic pain often unrelated to any schwannoma. Pathogenic variants of two genes, *SMARCB1* and *LZTR1*, are causal in familial cases. However, many schwannomatosis patients lack mutations in these genes. Surgery is the standard treatment for schwannomas but leaves patients with increasing neurological deficits. Pain management is a daily struggle controlled by the use of multiple analgesic and anti-inflammatory drugs. There is a need for both nonsurgical treatment to manage tumor growth and nonaddictive, nonsedative pain control. Because standard clinical trials are exceedingly difficult for patients with rare disorders, precision medicine approaches offer the possibility of bespoke therapeutic regimens to control tumor growth. As a proof of principle, we obtained a bio-specimen of paraspinal schwannoma from a schwannomatosis patient with a germline point mutation in the *SMARCB1/INI* gene. We created an *hTERT* immortalized cell line and tested the ability of targeted small molecules with efficacy in neurofibromatosis type 2–related schwannomas to reduce cell viability and induce cell death. We identified WP1066, a STAT3 inhibitor, currently in phase 2 clinical trials for pediatric and adult brain tumors as a lead compound. It reduced cell viability and STAT-3 phosphorylation and induced expression of markers for both necroptosis and caspase-dependent cell death. The results demonstrate feasibility in creating patient-derived cell lines for use in precision medicine studies.

Corresponding author:
cfv@ucf.edu

Ontology terms: chronic pain; neoplasm of the peripheral nervous system

Published by Cold Spring Harbor Laboratory Press

doi:10.1101/mcs.a006178

[Supplemental material is available for this article.]

INTRODUCTION

Schwannomatosis is a rare genetic schwannoma predisposition disorder (Koontz et al. 2013; Evans et al. 2018). It is characterized by the growth of benign schwannomas in peripheral, spinal, and, less frequently, cranial nerves. Schwannomatosis patients share similar clinical features with mosaic neurofibromatosis type 2 (NF2) patients that can make a differential diagnosis difficult (Louvrier et al. 2018). Both develop schwannomas, but only NF2 patients develop bilateral vestibular schwannomas (VSs), a diagnostic criterion for NF2. Another distinguishing feature of schwannomatosis is the presence of intractable, chronic neuropathic pain and intermittent intense pain when a tumor area is incidentally touched or palpated (Salar and Kaye 2020). Development of schwannomatosis symptoms can occur at any stage in life; however, it is most commonly diagnosed in early to mid-adulthood because of severe

pain or the presence of a single mass that upon imaging leads to visualization of multiple lesions along the spine (Merker et al. 2012). Management of the benign schwannomas varies depending upon their size and location. Schwannomas are often resected or debulked when associated with pain or tumor progression or when compromising nerve function. Commonly, pain management is a challenge for schwannomatosis patients, because they require multiple medications that affect activities of daily living (Farschtschi et al. 2020; Yohay and Bergner 2021). There is no specific class of analgesic found to be most effective in schwannomatosis (Yohay and Bergner 2021). Furthermore, there are no pharmacological treatments that consistently slow growth or promote regression of schwannomas in these patients.

Pathogenic variants of the *SMARCB1* (switch/sucrose nonfermentable [SWI/SNF]-related, matrix-associated, actin-dependent regulator of chromatin, subfamily B, member 1) and *LZTR1* (leucine zipper–like transcription regulator 1) genes occur in familial cases of schwannomatosis and in some but not all nonfamilial cases (Smith et al. 2012; Piotrowski et al. 2014; Paganini et al. 2015). The *SMARCB1* gene encodes a core subunit of the SWI/SNF chromatin remodeling complex involved in regulating cell proliferation and differentiation. Mutations in this gene are also linked to malignant rhabdoid tumors and sarcomas (Kohashi and Oda 2017; Vitte et al. 2017). The *LZTR1* gene encodes for a protein involved in ubiquitination and protein turnover including for those that regulate Ras/mitogen activated protein kinase (MAPK) signaling. Some pathogenic variants of this gene are associated with Noonan syndrome, a common RASopathy, as well as glioblastomas (Frattini et al. 2013; Steklov et al. 2018). The *NF2*, *SMARCB1*, and *LZTR1* genes are all located on Chromosome 22q11.21 to 12.2 within a span of 8.7 megabases (Tamura 2021). It is now widely accepted that schwannomatosis is caused by a "four hit-3" step inactivation of both *NF2* alleles and both alleles of *SMARCB1* and/or *LZTR1* (Sestini et al. 2008; Kehrer-Sawatzki et al. 2017).

The challenges in clinical management coupled with the rarity of the disease and its unknown genetic pathophysiology for many highlight the need for a precision medicine approach to improve care of individuals with schwannomatosis. Here, we provide a pilot drug screening study using a cell line created from a paraspinal schwannoma from a schwannomatosis patient with a point mutation in the *SMARCB1* gene. The well-documented medical history of this patient is typical for those with schwannomatosis and illustrates the struggle this syndrome poses for the patient and clinician.

RESULTS

Patient Clinical History

The clinical history highlights the diagnosis and interventions endured by the patient until an unexpected death due to a mesothelioma at age 38. A time line summarizing the patient's medical history is provided (Fig. 1). At the time of tumor donation, the patient was a 32-yr-old diagnosed with schwannomatosis suffering with severe neuropathic pain. Over a 15-yr period (age of 17 to age of 32), the patient underwent 20 surgical resections of peripheral and paraspinal schwannomas. The initial presentation was a lesion in the supraclavicular fossa that was excised at age of 17. By age 22, the patient had had seven procedures, including five laminectomies and Gamma Knife radiation therapy at the cervical 2–3 level. At age 24, genetic analyses performed on tumor tissue and blood lymphocytes did not reveal any pathogenic variants of the *NF1* and *NF2* genes. At age 28, genetic testing was conducted on a subsequent resected schwannoma, blood lymphocytes, and a mutation in *SMARCB1*; a newly identified causal schwannomatosis gene was identified (Table 1; Smith et al. 2012). The analyses revealed a germline point mutation in exon 8 of the *SMARCB1*

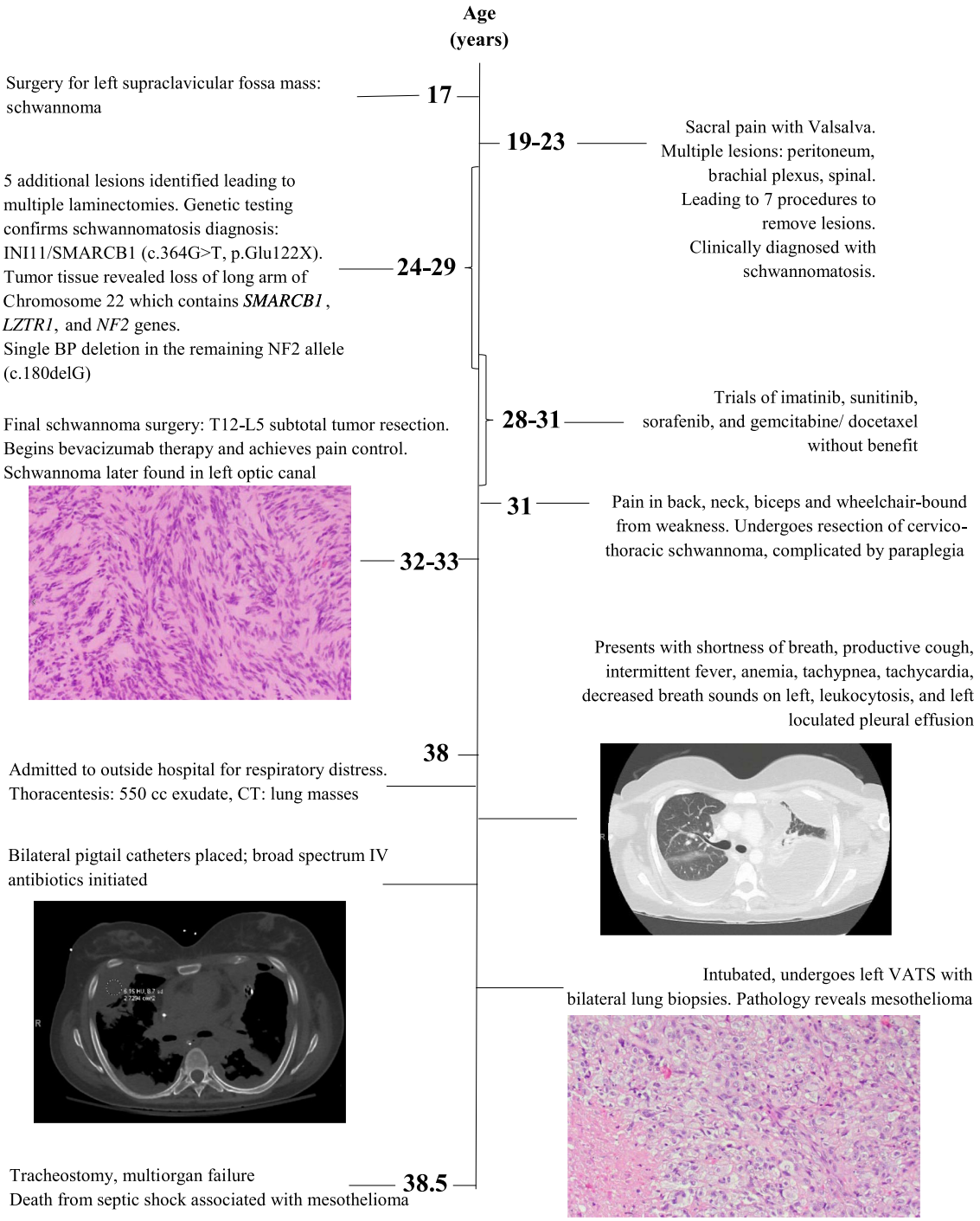

Figure 1. Time line summary of the patient's medical history.

gene; a guanine nucleotide was changed to a thymine at position 364 (c.364G > T (p. Glu122X)). The tumor tissue also had a total deletion of the long arm of Chromosome 22 (Chr 22:19,541,300–28,469,800) that includes the *SMARCB1*, *LZTR1*, and *NF2* genes, and

Table 1. Patient gene variant

Gene	Chromosome	HGVS DNA reference	HGVS protein reference	Variant type	Predicted effect	dbSNP/dbVar ID	Genotype
SMARCB1 OMIM 601607 NCBI 6598	22q11.23	c.364G > T	p.Glu122X	Missense	Substitution	NA	Heterozygous

a single base pair deletion in the remaining *NF2* allele (c.180delG). Additional paraspinal schwannoma resections between the ages of 28 and 31 left the patient paraplegic with upper extremity paresis.

At age 32, the patient began off-label infusions of bevacizumab (Avastin, Genentech-Roche), a recombinant humanized monoclonal antibody against vascular endothelial growth factor-A, because of a report of its success in decreasing pain in patients with neurofibromatosis (Linda and Recht 2016). With dosing every 21 d, remarkable pain control was achieved. The effect of bevacizumab on tumor shrinkage was not striking; however, the patient did not undergo additional schwannoma resections after initiation of bevacizumab therapy. Magnetic resonance imaging (MRI) of the spine and additional histology of schwannomas are shown (Supplemental Figs. S1 and S2). At age 33, the patient complained of worsening vision, and a lesion in the left optic canal was observed. The patient declined surgery and continued intermittent bevacizumab therapy for pain control.

At age 38, the patient was admitted to the hospital for worsening productive cough, dyspnea, and intermittent fevers and was soon placed on a ventilator. Although the patient had no known asbestos exposure, biopsies of lung lesions indicated a malignant mesothelioma. Mesothelioma is associated with inactivation of multiple genes including *NF2*, which is the second most common genetic alteration associated with mesothelioma (Sato and Sekido 2018; Cersosimo et al. 2021). The patient passed away at the age of 38 because of septic shock related to ongoing pulmonary infections associated with the malignant mesothelioma.

Characterization of the STSW-01 Cell Line

Primary and *hTERT* immortalized (STSW-01) schwannoma cells were characterized for proliferation requirements and marker expression. The cell morphology is seen in phase contrast images of dissociated primary tumor cells and the established cell lines (Fig. 2A; Supplemental Fig. S3). The primary schwannoma cells grew well and initially were elongated bipolar or multipolar cells and aligned with each other at high density. However, after the first passage, they became slow-growing large multipolar or amorphous cells that senesced by the second passage. Various growth factor combinations and laminin and CellBIND substrates were tested and did not alter their behavior (data not shown). Higher magnification images of schwannoma cells at passage 2 (P2) immunostained for various markers are shown (Supplemental Fig. S4). An h*TERT*-luciferase expressing line (STSW-01-*LUC*) was created for in vitro and in vivo studies and was studied in parallel with the hTERT line. Cells from both lines adhere well, are somewhat smaller than the primary cells, grow to a higher density without aligning, form multiple layers, and occasionally form cell aggregates. Growth assays were conducted to determine if STSW-01 proliferation was independent of external mitogens (Fig. 2B). Normal Schwann cells require both serum and mitogenic factors to proliferate in vitro (Iacovelli et al. 2007). The STSW-01 cells were capable of substantial proliferation in the absence of growth factors such as forskolin and sensory and motor neuron–derived factor (SMDF), a neuregulin isoform.

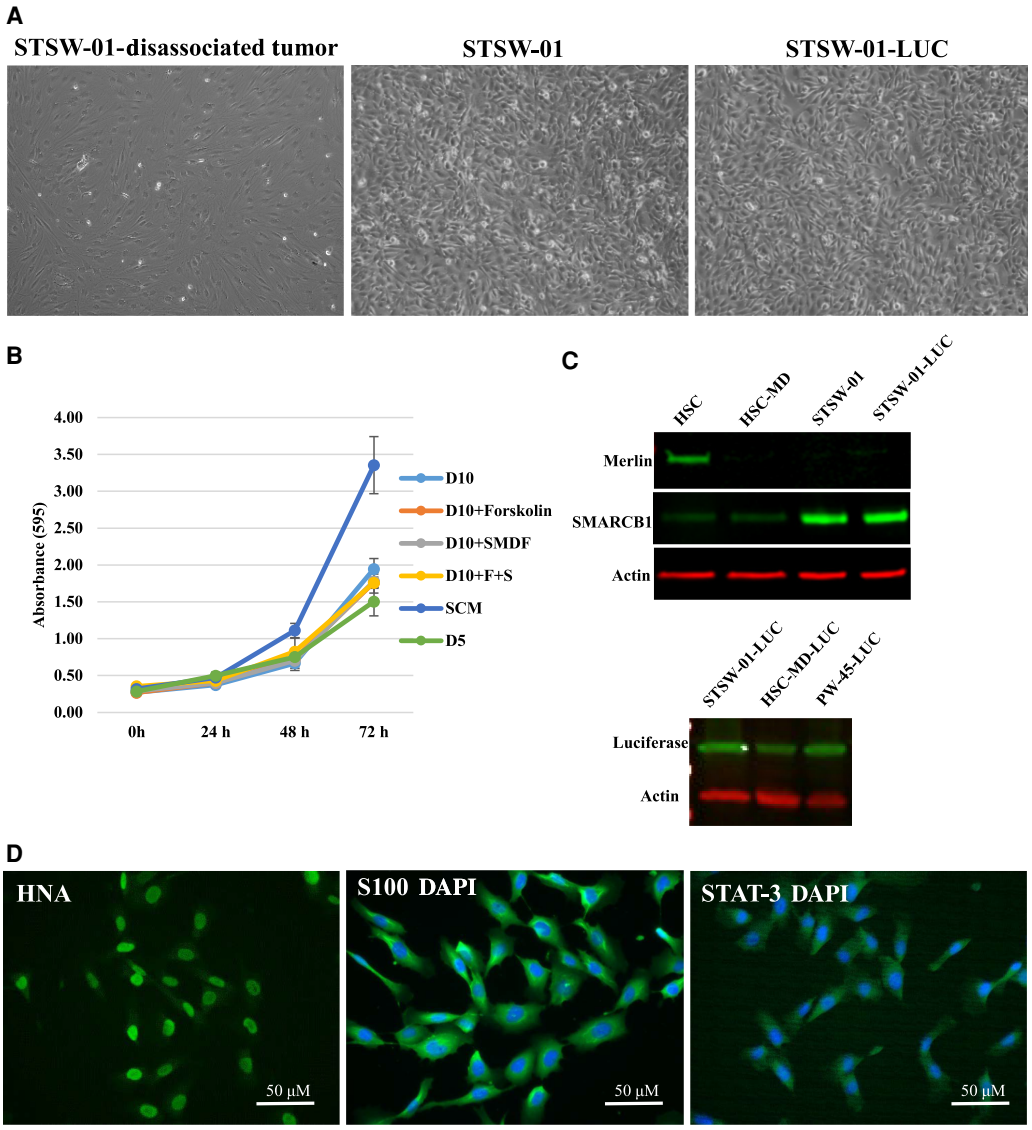

Figure 2. Characterization of STSW-01 cell lines. (*A*) Morphology of primary schwannoma cells and STSW-01 and STSW-01-LUC cells. (*B*) Proliferation assay comparing growth of STSW-01 cells in different growth media. (*C*) Western blots of both STSW-01 and STSW-01-LUC cells for merlin, SMARCB1, and luciferase. (*D*) Immunostaining of STSW-01 cells for indicated proteins. (HNA) Human nuclear antigen, (DAPI) 4′,6-diamidino-2-phenylindole.

Western blots indicate that the STSW-01 cells express high levels of the presumptive SMARCB1 pathogenic variant compared to human Schwann cells that are merlin-deficient (HSC-MD) and their isogenic normal Schwann cells (HSC). The STSW-01 cells did not express detectable levels of the NF2/merlin tumor suppressor (Fig. 2C). Immunostaining revealed that the cells expressed the Schwann cell marker S100, human nuclear antigen (HNA), STAT-3, platelet-derived growth factor receptor (PDGFR), vascular endothelial growth factor receptor 3 (VEGFR3), epidermal growth factor receptor (EGFR), rearranged during

transfection (RET; receptor for glial-cell line derived growth factor), phosphatase and tensin homolog (PTEN), SRC, and SRY-related HMG-box-10 (SOX-10) (Fig. 2D; Supplemental Figs. S4 and S5).

Functional Analyses Reveals That WP1066 Induces Necroptosis in STSW-01 Cells

The *hTERT* immortalized line transduced to express luciferase (STSW-01-*LUC*) was used to screen a small, curated drug library with the expectation of using this line for in vivo drug studies. Compounds were selected based on phosphokinase arrays of the primary schwannoma cells and genomic analyses of a previously resected schwannoma (Supplemental Fig. S6). The phospho-kinase arrays (R&D ARY003B) revealed high levels of pERK and pAKT in the primary schwannoma cells as well as those passaged once or twice in vitro. Other phosphorylated kinases detected were p53, p70 S6 kinase, PLC-g1, PYK2, p38a, CREB, AMPKα1, and β-catenin (Supplemental Fig. S6). Because the cells did not express the NF2/merlin tumor suppressor, we also tested the efficacy of multiple compounds that reduce the viability of several of our mouse and human NF2 model schwannoma cell lines (data not shown). Results of the viability assays identified active and inactive compounds (Fig. 3). Of the 14 compounds tested, 10 were considered active because they decreased cell viability in a dose-dependent manner by at least 60% with an IC_{50} ranging from 0.5 to 38 μM. Inactive compounds were those with a maximal efficacy <50% at the highest concentration tested. These included selumetinib, brigatinib, MK-0752, and sapitinib.

A dual cell death assay that measures binding to external annexin-V as an indicator of apoptosis and total cell death was conducted in the 384-well plate format during a 48-h incubation of STSW-01-*LUC* cells with active compounds at their respective IC_{50} or for WP1066 at the IC_{75}. WP1066 (3 μM) was the most effective compound at promoting membrane flipping when compared to other active compounds and was as effective as the positive control, staurosporine (2 μM; Fig. 3C). The peak signal occurred by 24 h of treatment. Only WP1066 promoted a time-dependent increase in overall cell death beginning by 20 h and increasing over time. To assess whether WP1066 modulated STAT3 activity, total cell lysates were prepared from STSW-01 and STSW-01-*LUC* cells incubated for 24 h with WP1066 at 1.5 and 3.0 μM. Western blots revealed that both cell lines had a 30%–50% decrease in pY705-STAT3 levels when grown in the presence of 3 μM WP1066 compared to DMSO controls (Fig. 4). A real-time caspase 3/7 activation assay was conducted to confirm induction of apoptosis. STSW-01-*LUC* cells plated in four to six replicates on 384 wells were treated with three concentrations of WP1066 and imaged over 48 h to capture phase images of cells and nuclear fluorescence of the cleaved caspase 3/7 probe. The proliferation rates of untreated and DMSO-treated wells were comparable. The slow increase in cleaved caspase 3/7-positive cells in control wells over time is likely due to nutrient depletion and/or overconfluence of the wells. The lower confluence of wells receiving 3 μM WP1066 coincided with the appearance of cleaved caspase 3/7 positive cells that began at 8 h of treatment and increased over time (Fig. 5A).

We explored whether necroptosis was induced by WP1066. Western blots were conducted for phosphorylated (Ser358) mixed lineage kinase domain–like (MLKL), a key protein activated by phosphorylation by receptor-interacting protein kinase 3 (RIPK3). Activation of MLKL leads to its translocation to the plasma membrane, where it forms pores causing cell death (Dhuriya and Sharm 2018). Total lysates of STSW-01 and STSW-01-*LUC* cells incubated with 1.5 and 3.0 μM WP1066 for 3 and 24 h were assessed for pMLKL (Ser358) levels and normalized to actin. A nearly threefold increase in pMLKL (50 kDa) compared to control levels was observed by 3 h of exposure to 1.5 and 3.0 μM WP1066 (Fig. 5B). Cleaved pMLKL (~25 kDa) was also observed in drug-treated cells. By 24 h of treatment, the levels of full-

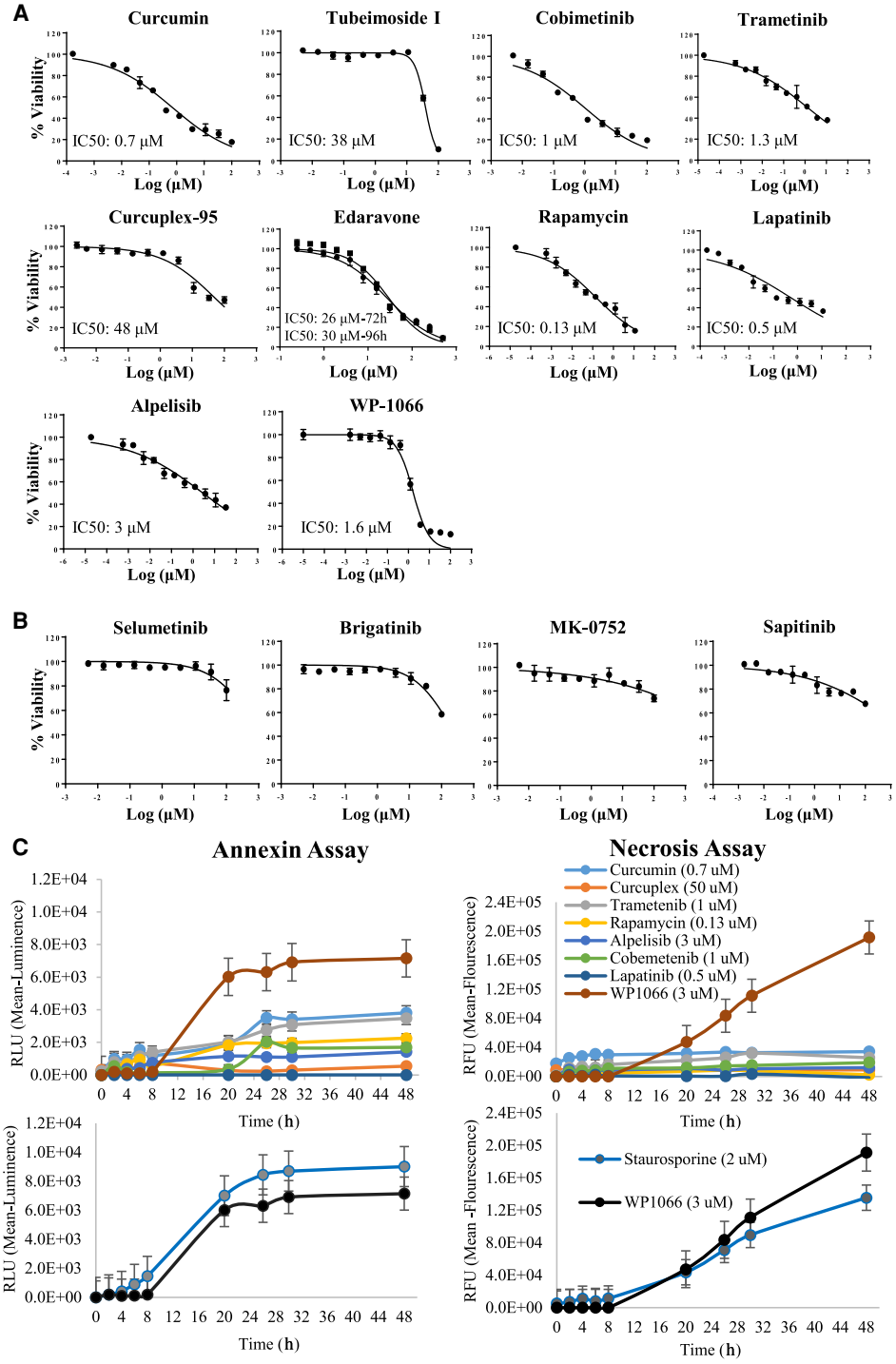

Figure 3. Viability curves for STSW-01-LUC cells treated with increasing doses of the indicated compounds. (*A*) active and (*B*) inactive compounds. (*C*) Forty-eight-hour annexin V and necrosis assays. (RLU) Relative light unit.

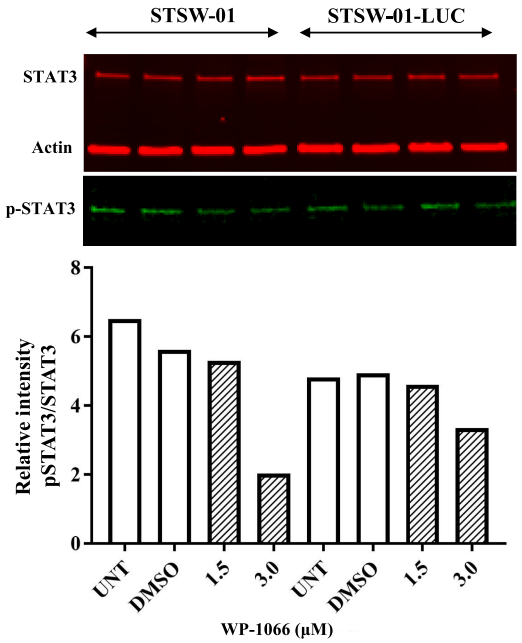

Figure 4. Western blots and quantitation for STAT3/p-STAT3 (Tyr 705) in both STSW-01 and STSW-01-LUC cells grown for 24 h in the presence of WP-1066.

length pMLKL did not differ significantly from controls (Fig. 5C); however, the levels of cleaved pMLKL remained elevated relative to the controls in both cell lines.

DISCUSSION

In this case study, we document the 22-yr struggle of a young individual with the rare genetic syndrome, schwannomatosis, to obtain clinical care and maintain a quality of life. A germline point mutation in the *SMARCB1* gene (c.364G > T) was the initial "hit" that led to development schwannomatosis with multiple schwannomas in peripheral, spinal, and cranial nerves and debilitating neuropathic pain. Multiple surgeries to remove paraspinal schwannomas resulted in paraplegia and did not lessen the pain that intensified over time. Multiple off-label drug regimens failed to control tumor growth. However, the anti-angiogenic biologic, bevacizumab, a humanized antibody against vascular endothelial growth factor, approved for recurrent glioblastoma and multiple other solid tumors, provided significant pain relief without significant tumor effects. The molecular mechanism by which bevacizumab diminishes pain is not well understood but significant pain control leading to cessation of pain medication has been reported within days of infusion in patients with neurofibromatosis types 2 and schwannomatosis (Blakeley et al. 2014; Linda and Recht 2016).

This is the second report of a schwannoma cell line derived from schwannomatosis patients. Two other schwannoma cell lines were created from a painful and a nonpainful schwannoma using SV40 virus large T antigen to immortalize the primary cells (Ostrow et al. 2015). SV40 has been associated with up-regulation of various genes and increased tumorigenicity, and it thus poses potential limitations in the usefulness of cell lines created with this method (Toouli et al. 2002). However, molecular comparison of parental and SV40 immortalized schwannoma cells using gene expression arrays did not uncover significant

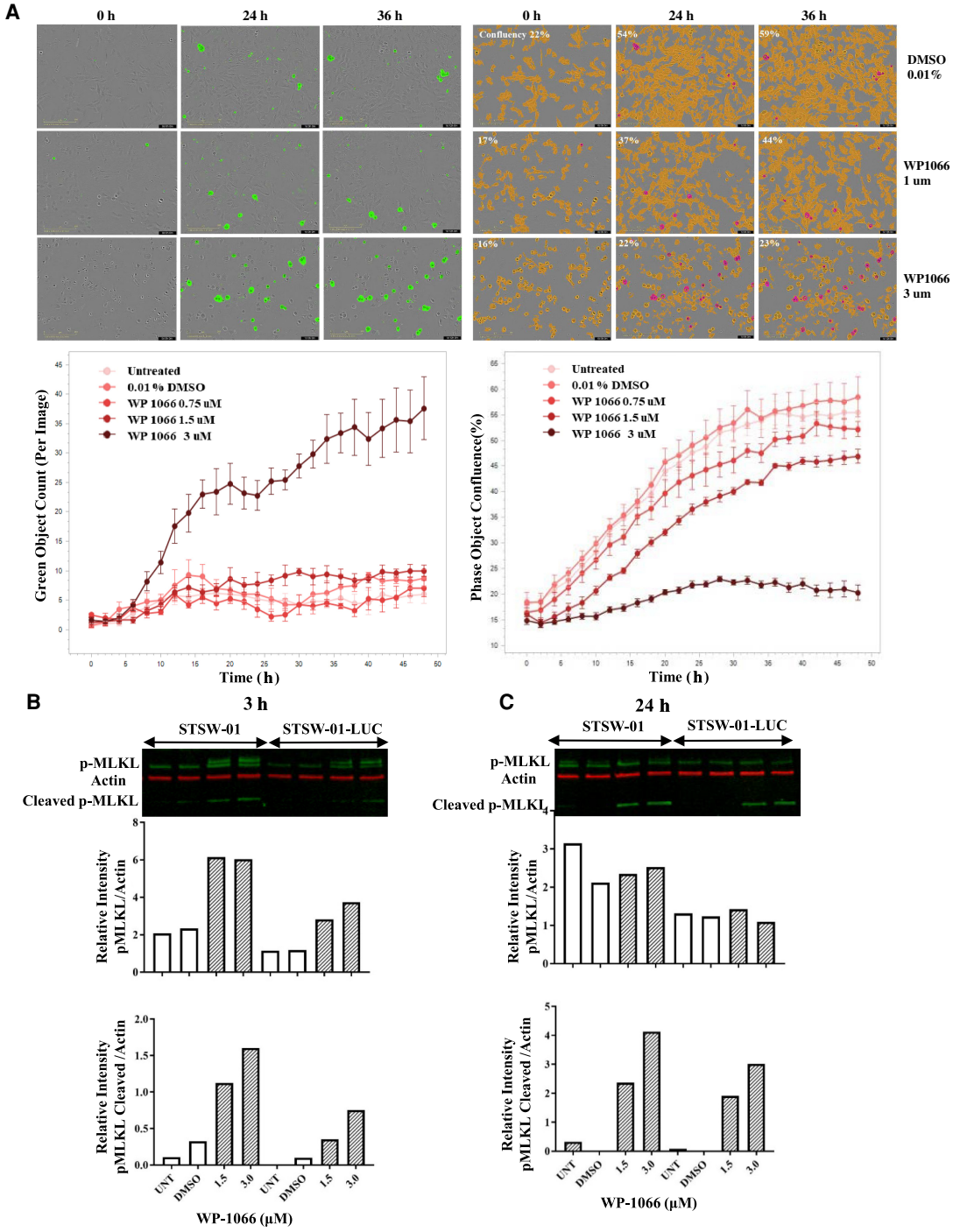

Figure 5. (*A*) Incucyte assay measuring well confluency and cleaved caspase 3/7 positive STSW-01-LUC cells grown in the presence of WP1066. Western blots for full-length and cleaved pMLKL (Ser358) in STSW-01 and STSW-01-LUC treated with WP1066 for (*B*) 3 h and (*C*) 24 h.

differences between the lines (Ostrow et al. 2015). The schwannoma cell lines reported here were immortalized using only *h-TERT* expression. The STSW-01 cells had significant expression of presumed nonfunctional SMARCB1, and merlin was not detected. The genetic analysis of a schwannoma resected from the patient at age 29 revealed inactivation of both *NF2* alleles. Thus, both paraspinal schwannomas resected at ages 29 and 32 were merlin-deficient according to genetic or western blot analyses. This is consistent with the current theory that schwannomas develop in schwannomatosis patients based on a four hit model that involves inactivation of *NF2* that drives tumor formation and inactivation of the *SMARCB1* or *LZTR1* genes that are associated with the pain syndrome (Sestini et al. 2008; Kehrer-Sawatzki et al. 2017). The patient's development of mesothelioma is likely related to *NF2* loss, as alterations in this gene have been found in 40% of mesothelioma patients (Sato and Sekido 2018). To our knowledge, this is the first report of a mesothelioma occurring in a schwannomatosis patient.

Of the 10 compounds that reduced viability of the STSW-01 cells, only WP1066 produced cytotoxicity. WP1066 decreased phosphorylation of STAT3 (Tyr 705) in a dose-dependent manner at 24 h; earlier time points were not studied. The NF2 tumor suppressor, merlin, has been shown to suppress activation of STAT3 in a human schwannoma cell line (Scoles et al. 2002). WP1066 is a JAK/STAT small molecule inhibitor that is in clinical trials in children and adults for various brain tumors (NCT04334863, NCT01904123). It has been shown to be effective in various cancer cell and mouse models and inhibits T regulatory cells (Hussain et al. 2007; Iwamaru et al. 2007; Kong et al. 2008; Koh et al. 2010; Heimberger 2011). It crosses the blood–brain barrier and modulates STAT3 activity as well as the activity of c-Myc and HIF-1α (Kong et al. 2009). Of note, CARIS Life Sciences profiling of a previously resected schwannoma identified elevated levels of HIF1α, c-KIT, and SRC mRNAs via microarray analysis. Activation and overexpression of these targets have been implicated in various malignancies (Sen and Johnson 2011; Stankov et al. 2014). Additional studies will confirm if these proteins were overexpressed in STSW-01 cells and if their levels or activities were modulated by WP1066.

Results of cell death studies suggest that WP1066 could directly induce necroptosis followed by induction of caspase 3/7-dependent apoptosis. Phosphorylated (Ser358) MLKL, indicative of late-stage necroptosis, was observed within 3 h of incubation of STSW-01 cells with 3 μM WP1066. By 24 h, the level of cleaved pMLKL remained high, yet full-length pMLKL levels were comparable to controls. The earliest appearance of cells expressing cleaved caspase 3/7 began at 8 h of WP1066 treatment, and their numbers increased over the next 40 h. Caspase-8 has been shown to cleave MLKL and initiate caspase 3/7–dependent apoptosis (Green and Llambi 2015). The induction of both apoptosis and necroptosis has been reported previously in hepatocellular carcinoma cell lines (Lin et al. 2016). We did not observe markers for autophagy (data not shown) in our studies. The molecular mechanism by which WP1066 triggers necroptosis and the link between the necroptotic and apoptotic pathways in this model requires further study.

STSW-01-cells expressing luciferase were assessed for their ability to grow as allografts in sciatic nerves of immune deficient NSG mice (Supplemental Fig. S7). A subset of cells survived engraftment but their slow and variable intraneural growth rate (threefold increase in radiance over 23 wk) was not amenable to in vivo drug efficacy studies. Patient-derived xenografts (PDXs) have been reported for *NF2* schwannomas using primary vestibular schwannoma cells and the HEI-193 cell line. HEI-193 cells were derived from an *NF2* patient schwannoma and immortalized with the human papilloma virus E6–E7 genes. The cells express merlin isoform 3 but not isoforms 1 and 2 (Hung et al. 2002). The HEI-193 cell line had a prolonged (6-wk) latent period before undergoing exponential growth over the last 4 wk of the study (Saydam et al. 2011). Only a small number of the primary vestibular schwannomas tested grew significantly in vivo (Chang et al. 2006). Future studies

will assess the efficacy of the investigational WP1066 drug delivered by intraperitoneal injection to immune-deficient mice implanted either subcutaneously or intraneurally with the STSW-01-*LUC* cell line. Adverse effects of the compound on normal nerves will also be evaluated.

This study reports methodology for establishing the first *hTERT* immortalized schwannoma cell line from a schwannomatosis patient. The cells proved amenable for drug screening in a high-content and high-throughput manner and led to identification of a cytotoxic compound currently in phase 1 clinical trials. The cell line can be used to screen libraries of FDA-approved drugs for repurposing for off-label use. Continued work in this area will further our understanding of how WP1066 leads to induction of two major cell death pathways, necroptosis and caspase-dependent apoptosis, in this patient-derived cell line. Our findings establish the framework for a precision medicine approach for improving care of schwannomatosis patients.

METHODS

Tumor Harvesting and Case Report

A schwannomatosis patient with a documented germline point mutation in the *SMARCB1* gene was consented using a University of Miami Institutional Review Board–approved protocol (#20120775) for tumor harvesting. The patient was also consented for derivation of a cell line for in vitro and in vivo studies as a case study designated as nonhuman subject research by University of Central Florida Institutional Review Board (IRB#00001138). The clinical presentation, clinical course, radiographic findings, tumor pathology, and genetic testing were reviewed as a case report with HIPAA compliance after the patient was deceased.

Antibodies

Beta-actin (8H10D10) and STAT3 (124H6) mouse antibodies and merlin (D1D8), phospho-STAT3 (Tyr705) (D3A7), SRC (2109), PDGFR (9360), and RET (14556) rabbit antibodies were purchased from Cell Signaling. The SMARCB1/SNF5 (A301-087A) antibody was purchased from Bethyl Laboratories. Anti-phospho-MLKL (17-10400), HNA (MAB1281), EGFR (NBP2-32843), and VEGFR3 (MAB3757) were purchased from Millipore Sigma. Anti-luciferase antibody (G7451) was purchased from Promega. Anti-S100 (GTX129573) antibody was purchased from GeneTex. Anti-PTEN (MA5-12278) antibody was purchased from ThermoFisher. Anti-SOX10 (Ab155279) antibody was purchased from Abcam.

Compounds

Curcumin (S1848), lapatinib (S2111), brigatinib (S8229), MK-0752 (S2660), sapitinib (S2192), and WP1066 (S2796) were all purchased from SellekChem. Cobimetinib (HY-13064), selumetinib (HY-50706), alpelisib (HY-15244), and trametinib (HY-10999) were purchased from MedChemExpress. Rapamycin (SC3504A) was acquired from SantaCruz Biotechnology and curcuplex-95 from Xymogen.

Cell Line

In the operating room, the schwannoma was immediately placed in chilled L15 medium and transported to the laboratory. The tumor was minced into small pieces (~1 mm), distributed into multiple vials, and frozen in cell culture freezing medium (90% heat-inactivated fetal bovine serum (FBS), 10% dimethyl sulfoxide (DMSO)). Schwannoma cells were isolated from individual vials and cultured on laminin-coated dishes in Dulbecco's modified Eagle medium

(DMEM) supplemented with 10% FBS, 10 ng/mL neuregulin (R&D 378-SM-025), 5 ng/mL fibroblast growth factor (Thermo Fisher), and 2 μM forskolin (Sigma-Aldrich). The freshly dissociated cells initially grew well but senesced after two passages. Schwannoma cells from a subsequent vial were immortalized by viral transduction with human telomerase gene (hTERT lentivirus, CMV, Puromycin; Cellomics Technology) to establish a cell line referred to as STSW-01. For in vivo experiments, STSW-01 cells were transduced with the firefly luciferase (CMV, neomycin lentivirus; Kerafast) to establish a cell line referred to as STSW-01-LUC. The cell lines were routinely cultured on CellBIND (Corning) dishes in Schwann cell media (SCM, ScienCell 1701) containing HEPES buffer and bicarbonate buffered basal medium with 5% FBS, penicillin/streptomycin, and a proprietary supplement mix containing platelet-derived growth factor (PDGF), glial growth factor (GGF), forskolin, phorbol 12-myristate 13-acetate (PMA), putrescine, selenium, insulin, insulin growth factor-1 (IGF-1), hydrocortisone, and T3 thyroid hormone. Cultures were incubated at 37°C with 5% CO_2 and passaged when ~80% confluent.

Viability Assays

Viability assays were conducted using 384-well CellBIND plates. STSW-01-LUC cells grown in SCM were plated at a density of 5000/18 μL/well. The cells were incubated for 4 h to allow cell attachment. Compounds (2 μL) dissolved in DMSO were added in triplicate wells over a range of nine concentrations, and DMSO (0.1%) was used as a control. The plates were spun and incubated for 48 h at 37°C with 5% CO_2. The medium was removed, and 20 μL of CellTiter-Flour reagent in assay buffer (CellTiter-Fluor, Promega) was added to wells and incubated for 45 min. Fluorescence was quantified using a Synergy Microplate Reader (BioTek).

Annexin V and Necrosis Assays

Annexin V and necrosis assays were conducted on 384-well plates with 2000 cells in 15 μL per well. Cells grew for 24 h in SCM before adding compounds. The annexin and necrosis detections reagents were added to the wells following manufacturer's recommended protocol for the RealTime-Glo assay (Promega JA1000, JA1001). Luminescence and fluorescent values for each well were recorded over a 48-h time period using a Synergy Microplate Reader (BioTek).

Western Blot

Cells were lysed using Laemmli extraction buffer to obtain total cellular proteins. Lysates were boiled for 5 min and stored at −80°C. Equal volume of lysates were loaded on 4%–20% precast polyacrylamide gels (Bio-Rad) and run at 200 V for 40 min. Proteins were transferred onto polyvinylidene fluoride (PVDF) membranes (Immobilon-FL; Millipore) at 100 V for 1 h at 4°C. Membranes were blocked with 1:1 Odyssey blocking buffer (Licor)/1× tris buffered saline (TBS) and incubated with primary antibodies overnight at 4°C. Secondary antibodies were added at 1:25,000 dilution and were incubated for 45 min. Membranes were washed after primary and secondary antibodies with 1× TBS with Tween three times for 10 min. Membranes were imaged using the LI-COR Biosciences Odyssey Infrared Imaging System and quantified via Odyssey Image Studio.

Incucyte Live Imaging/Caspase 3/7 Cleavage Assay

STSW-01-LUC cells were seeded in SCM on a 384-well plate (1000 cells/15 μL in SCM) and allowed to attach and grow overnight (12–16 h) at 37°C. The Incucyte Caspase-3/7 Green Apoptosis Assay reagent was added at 5 uM final concentration and followed by compound addition in four replicates per condition. The plate was briefly centrifuged and placed in the

Incucyte live imaging system inside the incubator and imaged for 48 h. Phase and fluorescent images were captured at 4-h increments. Analysis of well confluency and number of green-labeled nuclei was performed using the Incucyte Basic Analyzer software.

Immunostaining

Immunofluorescent staining was carried out on STSW-01 cells grown to 80% confluency in 96-well plates. Wells were washed with phosphate buffered saline (PBS) before fixing in 4% paraformaldehyde for 10 min and permeabilized using 0.1% triton X-100. Wells were washed and nonspecific staining blocked with 5% normal goat serum and PBS for 30 min. Wells were incubated overnight at 4°C with primary antibody in blocking buffer at the recommended antibody dilutions. Alexa Flour secondary antibodies were used at 1:200 with 4′,6-diamidino-2-phenylindole (DAPI) nuclear stain (Thermo Fisher D3571) at 1:250 in blocking buffer and incubated for 45 min. The cells were washed and postfixed in 4% paraformaldehyde. Wells were imaged on a Keyence BZ-X800 microscope.

ADDITIONAL INFORMATION

Data Deposition and Access

Variant information has been uploaded to the Human Genomic Mutation Database at http://www.hgmd.cf.ac.uk/ac/index.php. The variant was submitted to ClinVar (https://www.ncbi.nlm.nih.gov/clinvar/) and can be found under accession number VCV001076272.3.

Ethics Statement

Patient consent for tumor harvesting was performed under a University of Miami Institutional Review Board–approved protocol (#20120775). Patient consent for derivation of a cell line for in vitro and in vivo studies as a case study was designated as nonhuman subject research by University of Central Florida Institutional Review Board (IRB#00001138). Written consent from the patient's family to publish this case study was obtained.

Acknowledgments

We thank the patient and family for willingness to donate tissue for preclinical studies, share medical history, and provide support through Genes Foundation and Passion For The Sun. We thank Drs. R. Komotar and A. Bregy (Department of Neurological Surgery at University of Miami Miller School of Medicine) for patient consent through UMMSM Brain Tumor Bank, Dr. Monje (The Miami Project to Cure Paralysis) for assistance with sample processing, Dr. L.-S. Chang for sharing his hTERT immortalization protocol, Dr. S. Lambert for editing the manuscript, and Barbara Franklin for suggesting the use of WP1066.

The patient is identified at the family's request. Katherin Mireya Sabbagh lived her life between reality and hope. She knew her struggle would benefit others in some way and this purpose fueled her daily struggle. Her desire to leave a legacy lit the flame of her life. Katherin Mireya Sabbagh vivió su vida entre una realidad y una esperanza. Sabía que su lucha era para beneficiar a otros de una u otra forma. Entre la realidad y la esperanza encontró su propósito que le daba fuerzas para seguir luchando y su visión de dejar un legado prendía la llama de su vida.

Author Contributions

A.A., B.V., and R.R. designed, conducted, and analyzed experiments; A.A. designed figures and wrote the first draft; and C.M., S.H.G., and C.T.D. reviewed clinical history, designed figures, and participated in writing. C.F.-V. conceived of the project, designed the experiments,

Competing Interest Statement

The authors have declared no competing interest.

Referees

D. Gareth Evans
Anonymous

Received December 15, 2021; accepted in revised form April 8, 2022.

and analyzed results and wrote subsequent versions of manuscript. All authors commented on the manuscript.

Funding

Support was provided by the National Institutes of Health grant R01DC017264 to C.F.-V. and Xue-Zhong-Liu and 1R56NS102254 to C.F.-V.

REFERENCES

Blakeley J, Schreck KC, Evans DG, Korf BR, Zagzag D, Karajannis MA, Bergner AL, Belzberg AJ. 2014. Clinical response to bevacizumab in schwannomatosis. *Neurology* **83:** 1986–1987.

Cersosimo F, Barbarino M, Lonardi S, Vermi W, Giordano A, Bellan C, Giurisato E. 2021. Mesothelioma malignancy and the microenvironment: molecular mechanisms. *Cancers (Basel)* **13:** 5664. doi:10.3390/cancers13225664

Chang LS, Jacob A, Lorenz M, Rock J, Akhmametyeva EM, Mihai G, Schmalbrock P, Chaudhury AR, Lopez R, Yamate J, et al. 2006. Growth of benign and malignant schwannoma xenografts in severe combined immunodeficiency mice. *Laryngoscope* **116:** 2018–2026. doi:10.1097/01.mlg.0000240185.14224.7d

Dhuriya YK, Sharm D. 2018. Necroptosis: a regulated inflammatory mode of cell death. *J Neuroinflammation* **15:** 199. doi:10.1186/s12974-018-1235-0

Evans DG, Bowers NL, Tobi S, Hartley C, Wallace AJ, King AT, Lloyd SKW, Rutherford SA, Hammerbeck-Ward C, Pathmanaban ON, et al. 2018. Schwannomatosis: a genetic and epidemiological study. *J Neurol Neurosurg Psychiatry* **89:** 1215–1219. doi:10.1136/jnnp-2018-318538

Farschtschi SC, Mainka T, Glatzel M, Hannekum AL, Hauck M, Gelderblom M, Hagel C, Friedrich RE, Schuhmann MU, Schulz A, et al. 2020. C-fiber loss as a possible cause of neuropathic pain in schwannomatosis. *Int J Mol Sci* **21:** 3569. doi:10.3390/ijms21103569

Frattini V, Trifonov V, Chan JM, Castano A, Lia M, Abate F, Keir ST, Ji AX, Zoppoli P, Niola F, et al. 2013. The integrated landscape of driver genomic alterations in glioblastoma. *Nat Genet* **45:** 1141–1149. doi:10.1038/ng.2734

Green DR, Llambi F. 2015. Cell death signaling. *Cold Spring Harb Perspect Biol* **7:** a006080. doi:10.1101/cshperspect.a006080

Heimberger AB. 2011. The therapeutic potential of inhibitors of the signal transducer and activator of transcription 3 for central nervous system malignancies. *Surg Neurol Int* **2:** 163. doi:10.4103/2152-7806.89886

Hung G, Li X, Faudoa R, Xeu Z, Kluwe L, Rhim JS, Slattery W, Lim D. 2002. Establishment and characterization of a schwannoma cell line from a patient with neurofibromatosis 2. *Int J Oncol* **20:** 475–482.

Hussain SF, Kong LY, Jordan J, Conrad C, Madden T, Fokt I, Priebe W, Heimberger AB. 2007. A novel small molecule inhibitor of signal transducers and activators of transcription 3 reverses immune tolerance in malignant glioma patients. *Cancer Res* **67:** 9630–9636. doi:10.1158/0008-5472.CAN-07-1243

Iacovelli J, Lopera J, Bott M, Baldwin E, Khaled A, Uddin N, Fernandez-Valle C. 2007. Serum and forskolin cooperate to promote G1 progression in Schwann cells by differentially regulating cyclin D1, cyclin E1, and p27Kip expression. *Glia* **55:** 1638–1647. doi:10.1002/glia.20578

Iwamaru A, Szymanski S, Iwado E, Aoki H, Yokoyama T, Fokt I, Hess K, Conrad C, Madden T, Sawaya R, et al. 2007. A novel inhibitor of the STAT3 pathway induces apoptosis in malignant glioma cells both *in vitro* and *in vivo*. *Oncogene* **26:** 2435–2444. doi:10.1038/sj.onc.1210031

Kehrer-Sawatzki H, Farschtschi S, Mautner VF, Cooper DN. 2017. The molecular pathogenesis of schwannomatosis, a paradigm for the co-involvement of multiple tumour suppressor genes in tumorigenesis. *Hum Genet* **136:** 129–148. doi:10.1007/s00439-016-1753-8

Koh MY, Spivak-Kroizman TR, Powis G. 2010. HIF-1α and cancer therapy. *Recent Results Cancer Res* **180:** 15–34. doi:10.1007/978-3-540-78281-0_3

Kohashi K, Oda Y. 2017. Oncogenic roles of SMARCB1/INI1 and its deficient tumors. *Cancer Sci* **108:** 547–552. doi:10.1111/cas.13173

Kong LY, Abou-Ghazal MK, Wei J, Chakraborty A, Sun W, Qiao W, Fuller GN, Fokt I, Grimm EA, Schmittling RJ, et al. 2008. A novel inhibitor of signal transducers and activators of transcription 3 activation is efficacious against established central nervous system melanoma and inhibits regulatory T cells. *Clin Cancer Res* **14:** 5759–5768. doi:10.1158/1078-0432.CCR-08-0377

Kong LY, Wei J, Sharma AK, Barr J, Abou-Ghazal MK, Fokt I, Weinberg J, Rao G, Grimm E, Priebe W, et al. 2009. A novel phosphorylated STAT3 inhibitor enhances T cell cytotoxicity against melanoma through

inhibition of regulatory T cells. *Cancer Immunol Immunother* **58:** 1023–1032. doi:10.1007/s00262-008-0618-y

Koontz NA, Wiens AL, Agarwal A, Hingtgen CM, Emerson RE, Mosier KM. 2013. Schwannomatosis: the overlooked neurofibromatosis? *AJR Am J Roentgenol* **200:** W646–W653.

Lin CY, Chang TW, Hsieh WH, Hung MC, Lin IH, Lai SC, Tzeng YJ. 2016. Simultaneous induction of apoptosis and necroptosis by Tanshinone IIA in human hepatocellular carcinoma HepG2 cells. *Cell Death Discov* **2:** 16065. doi:10.1038/cddiscovery.2016.65

Linda XW, Recht LD. 2016. Bevacizumab for treatment-refractory pain control in neurofibromatosis patients. *Cureus* **8:** e933. doi:10.7759/cureus.933

Louvrier C, Pasmant E, Briand-Suleau A, Cohen J, Nitschké P, Nectoux J, Orhant L, Zordan C, Goizet C, Goutagny S, et al. 2018. Targeted next-generation sequencing for differential diagnosis of neurofibromatosis type 2, schwannomatosis, and meningiomatosis. *Neuro Oncol* **20:** 917–929. doi:10.1093/neuonc/noy009

Merker VL, Esparza S, Smith MJ, Stemmer-Rachamimov A, Plotkin SR. 2012. Clinical features of schwannomatosis: a retrospective analysis of 87 patients. *Oncologist* **17:** 1317–1322. doi:10.1634/theoncologist.2012-0162

Ostrow KL, Donaldson K, Blakeley J, Belzberg A, Hoke A. 2015. Immortalized human Schwann cell lines derived from tumors of schwannomatosis patients. *PLoS ONE* **10:** e0144620. doi:10.1371/journal.pone.0144620

Paganini I, Chang VY, Capone GL, Vitte J, Benelli M, Barbetti L, Sestini R, Trevisson E, Hulsebos TJ, Giovannini M, et al. 2015. Expanding the mutational spectrum of *LZTR1* in schwannomatosis. *Eur J Hum Genet* **23:** 963–968. doi:10.1038/ejhg.2014.220

Piotrowski A, Xie J, Liu YF, Poplawski AB, Gomes AR, Madanecki P, Fu C, Crowley MR, Crossman DK, Armstrong L, et al. 2014. Germline loss-of-function mutations in *LZTR1* predispose to an inherited disorder of multiple schwannomas. *Nat Genet* **46:** 182–187. doi:10.1038/ng.2855

Salar M, Kaye MB. 2020. Multiple schwannomas of the median nerve: a case report and review of the literature. *J Orthop Case Rep* **10:** 60–63. doi:10.13107/jocr.2020.v10.i06.1876

Sato T, Sekido Y. 2018. NF2/Merlin inactivation and potential therapeutic targets in mesothelioma. *Int J Mol Sci* **19:** 988. doi:10.3390/ijms19040988

Saydam O, Ozdener GB, Senol O, Mizrak A, Prabhakar S, Stemmer-Rachamimov AO, Breakefield XO, Brenner GJ. 2011. A novel imaging-compatible sciatic nerve schwannoma model. *J Neurosci Methods* **195:** 75–77. doi:10.1016/j.jneumeth.2010.10.021

Scoles DR, Nguyen VD, Qin Y, Sun CX, Morrison H, Gutmann DH, Pulst SM. 2002. Neurofibromatosis 2 (NF2) tumor suppressor schwannomin and its interacting protein HRS regulate STAT signaling. *Hum Mol Genet* **11:** 3179–3189. doi:10.1093/hmg/11.25.3179

Sen B, Johnson FM. 2011. Regulation of SRC family kinases in human cancers. *J Signal Transduct* **2011:** 865819. doi:10.1155/2011/865819

Sestini R, Bacci C, Provenzano A, Genuardi M, Papi L. 2008. Evidence of a four-hit mechanism involving *SMARCB1* and *NF2* in schwannomatosis-associated schwannomas. *Hum Mutat* **29:** 227–231. doi:10.1002/humu.20679

Smith MJ, Wallace AJ, Bowers NL, Rustad CF, Woods CG, Leschziner GD, Ferner RE, Evans DG. 2012. Frequency of SMARCB1 mutations in familial and sporadic schwannomatosis. *Neurogenetics* **13:** 141–145. doi:10.1007/s10048-012-0319-8

Stankov K, Popovic S, Mikov M. 2014. C-KIT signaling in cancer treatment. *Curr Pharm Des* **20:** 2849–2880. doi:10.2174/13816128113199990593

Steklov M, Pandolfi S, Baietti MF, Batiuk A, Carai P, Najm P, Zhang M, Jang H, Renzi F, Cai Y, et al. 2018. Mutations in LZTR1 drive human disease by dysregulating RAS ubiquitination. *Science* **362:** 1177–1182. doi:10.1126/science.aap7607

Tamura R. 2021. Current understanding of neurofibromatosis type 1, 2, and schwannomatosis. *Int J Mol Sci* **22:** 5850. doi:10.3390/ijms22115850

Toouli CD, Huschtscha LI, Neumann AA, Noble JR, Colgin LM, Hukku B, Reddel RR. 2002. Comparison of human mammary epithelial cells immortalized by simian virus 40 T-antigen or by the telomerase catalytic subunit. *Oncogene* **21:** 128–139. doi:10.1038/sj.onc.1205014

Vitte J, Gao F, Coppola G, Judkins AR, Giovannini M. 2017. Timing of *Smarcb1* and *Nf2* inactivation determines schwannoma versus rhabdoid tumor development. *Nat Commun* **8:** 300. doi:10.1038/s41467-017-00346-5

Yohay K, Bergner A. 2021. Schwannomatosis. In *UpToDate* (ed. Post TW). UpToDate, Waltham, MA.